Ergod. Th. & Dynam. Sys. (2006), **26**, 1749–1768
doi:10.1017/S0143385706000484
© *2006 Cambridge University Press*
Printed in the United Kingdom

A hyperelliptic realization of the horseshoe and baker maps

R. CHAMANARA†, F. P. GARDINER‡ and N. LAKIC§

† *Department of Mathematics, Indiana University, Bloomington, IN 47405, USA*
(e-mail: rchamana@indiana.edu)
‡ *Department of Mathematics, Brooklyn College, Brooklyn, NY 11210, USA*
(e-mail: fgardiner@gc.cuny.edu)
§ *Department of Mathematics, Herbert H. Lehman College, Bronx, NY 10468, USA*
(e-mail: nlakic@lehman.cuny.edu)

(*Received* 27 *October* 2005 *and accepted in revised form* 27 *June* 2006)

Abstract. We present a generalization of the functional equation for the Weierstrass $\wp$-function for hyperelliptic surfaces of infinite genus arising from iteration of the horseshoe and baker maps. The ramified cover of these infinite genus surfaces over the complex plane are associated to a quadratic differential of finite norm with simple poles accumulating to infinity. We study the geometry of its critical trajectories emanating from these poles and their rate of accumulation.

0. *Introduction*

In discrete time dynamics, a basic topic of study is the repeated application of a self-mapping f of a Hausdorff topological space X. In our case we let $\tilde{X}$ be the unit square $\{z = x + iy : 0 \leq x \leq 1, 0 \leq y \leq 1\}$ minus a set $\mathcal{S}$, where $\mathcal{S}$ is a countable set on the boundary with one accumulation point at the origin. Then X is $\tilde{X}$ factored by an equivalence relation obtained by certain identifications along its sides. The equivalence classes are chosen so that a particular discontinuous self mapping $\tilde{f}$ of $\tilde{X}$ induces an Anosov-like homeomorphism f of the factor space $X = \tilde{X}/\sim$. It will turn out that in one case we can view all of the elements of $\mathcal{S}$ as forming another equivalence class, and by adding that equivalence class to X we obtain the Riemann sphere.

We carry out this construction in two cases, one for the baker map and one for the horseshoe map. We find that the first case yields a Riemann surface Y of infinite genus together with a conformal involution c such that $\pi : Y \to Y/c \cong X$ is a two-to-one ramified cover of a surface of genus zero given by the second case. The cover $Y \to Y/c$ has infinitely many ramified points of order two whose images in X accumulate to an isolated point, and up to postcomposition by a complex affine transformation, $z \mapsto az + b$,

https://doi.org/10.1017/S0143385706000484 Published online by Cambridge University Press

X is realizable uniquely as a domain in the complex plane $\mathbb{C}$. The self-mapping f of X extends continuously to the conformal completion of X and acts as a shift map on the images of the ramified points. Under the covering $\pi : Y \to Y/c$ there is an extremal Anosov-like self-mapping F of Y such that $\pi \circ F = f \circ \pi$ and such that the dilatation of F is constantly equal to 4. In [**3**] it is shown that the Riemann surface Y decomposes into an infinite family of Jenkins–Strebel annuli in different ways, and the extremal mapping F is a composition of two multi-Dehn twists associated to two of these ways.

By Koebe uniformization there is a conformal mapping z that maps X to the complex plane and that extends to the ramification points with the property that these points accumulate to ∞. If ζ is the natural parameter of the unit square $\tilde{X}$, then the holomorphic function

$$w(\zeta) = dz/d\zeta \tag{1}$$

is well defined on Y, and w^2 is a well-defined function of z in X. If p_j is one of the ramification points on the boundary of $\tilde{X}$, by definition we let $a_j = z(p_j)$. We find a sequence of hyperelliptic Riemann surfaces Y_n of genus n covering the Riemann sphere with $2n + 2$ points removed defined by equations

$$w_n^2(z_n) = z_n \prod_{|j|=1}^{n} (1 - z_n/a_{jn}) \tag{2}$$

that converge to the Riemann surface Y of infinite genus in the following sense. The holomorphic functions z_n and w_n converge locally uniformly to z and w and the points a_{jn} converge to a_j as $n \to \infty$. Moreover, the quadratic differentials

$$\frac{(dz_n)^2}{z_n \prod_{|j|=1}^{n}(1 - z_n/a_{jn})} \tag{3}$$

converge in the L_1-norm to the quadratic differential $(dz)^2/w^2$. We also give an estimate for the rate at which the points a_j approach ∞ as $j \to \pm\infty$. The quadratic differential $(dz)^2/w^2$ has horizontal trajectories leading from simple poles at the points a_j to the umbilic point at ∞. With respect to a conformal local parameter vanishing at ∞, these trajectories all approach the umbilic point at zero angle. Moreover, there are positive constants C and α such that $|a_j| \geq C|j|^\alpha$.

Finally, we give a method for finding a quasiconformal homeomorphism $\zeta \mapsto \tilde{z}$ from X onto $\mathbb{C}$, so that z is a quasiconformal function of $\tilde{z}$. The method gives an explicit form of the Beltrami coefficient so that a computer program should make it possible to calculate this homeomorphism. Since quasiconformal maps are Hölder continuous and since the map involves taking a logarithm at the umbilic point, we will see that the poles a_j cannot converge to ∞ geometrically. That is, there cannot exist constants $C > 0$ and $\lambda > 1$ such that $|a_j| > C\lambda^j$.

The paper is organized as follows. In the first section we show how by cutting along horizontal segments in a square and pasting by translations and rotations through 180° along horizontal and vertical subintervals of the sides of the square, one can realize a topological version of the horseshoe map as a homeomorphism of a surface X of genus zero. This construction was shown to us by André de Carvalho. We also show how the

https://doi.org/10.1017/S0143385706000484 Published online by Cambridge University Press

baker map is realized by a homeomorphism of the square with similar side identifications that involve the use of translations only, but that yield a surface Y of infinite genus, which is a double cover of X.

In §2 we calculate the genus of a surface obtained by identifying finitely many pairs of parallel segments that comprise the sides of a rectangle in the ζ-plane. In this section we assume that all of the side pairings are realized by translations and we calculate the order of the zero or zeros of the associated abelian differential $d\zeta$.

The third section concerns the hyperelliptic relationship between finite surfaces X_{nm} and Y_{nm} discussed in §2. After a suitable normalization, there is a unique Koebe map $\zeta \mapsto z_{nm}$ from X_{nm} onto $\mathbb{C}$ with the property that $w_{nm} = dz_{nm}/d\zeta$ is well defined on Y_{nm} and w_{nm}^2 is a function of z_{nm}. In fact, by comparing orders of the zeros at the images of the hinge points and at ∞, we find that $w_{nm}^2(z_{nm})$ is the polynomial in z_{nm} given by

$$w_{nm}^2(z_{nm}) = z_{nm} \prod_{k=1}^{n} (1 - z_{nm}/a_{kn}) \prod_{j=1}^{m} (1 - z_{nm}/b_{jn}). \tag{4}$$

In §4 we return to the dynamically generated examples discussed in §1 and derive an estimate that gives a lower bound on the rate at which the images of the hinge points of X converge to ∞. By using this result in §5 we are able to show the L_1-convergence referred to in formula (3).

In §6 we exploit the action of the natural conformal injection of an open subset of X into itself induced by the map $\zeta \mapsto (1/2)\zeta$. By considering the effect of this map we show that the critical horizontal and vertical trajectories of the quadratic differential $(d\zeta)^2$ lead to the umbilic point at zero angle.

In §7 we construct a map $\zeta \mapsto \tilde{z}$ from X to $\mathbb{C}$ such that z is a quasiconformal function of $\tilde{z}$. This construction shows that images of the hinge points converge to the umbilic point radially and they cannot converge geometrically. This stands in contrast to the approach towards the umbilic point of the critical vertical and horizontal trajectories. These critical trajectories approach at zero angle and from the side opposite the approach of the hinge points.

We would like to thank the referee for several helpful corrections and modifications.

1. *Dynamically generated Riemann surfaces*

1.1. *The horseshoe example.* Here we describe the horseshoe self-map $\tilde{f}$ of $\tilde{X}$ in two steps. The description follows exactly a recipe shown to us by André de Carvalho. See [**4**] for a description of a large family of similar examples corresponding to different topological classes of homeomorphisms of the sphere. The first step is to cut $\tilde{X}$ along the line segment $y = \frac{1}{2}, 0 < x < 1$ into two parts: the upper part X_1, and the lower part X_0. We turn over the upper part X_1 and then translate it so that it fits contiguously next to the right side of X_0. Explicitly, points z in X_0 remain unmoved and points z in X_1 are moved to $L(z) = -z + 2 + i$. Thus $X_0 \cup L(X_1)$ is a rectangle with its bottom side along the horizontal interval from $x = 0$ to $x = 2$ and with its left vertical side along the interval from $y = 0$ to $y = \frac{1}{2}$. The second step is to apply the map $z = x + iy \mapsto (\frac{1}{2})x + 2iy$. By definition, $\tilde{f}$ is given by the composition of these two steps.

https://doi.org/10.1017/S0143385706000484 Published online by Cambridge University Press

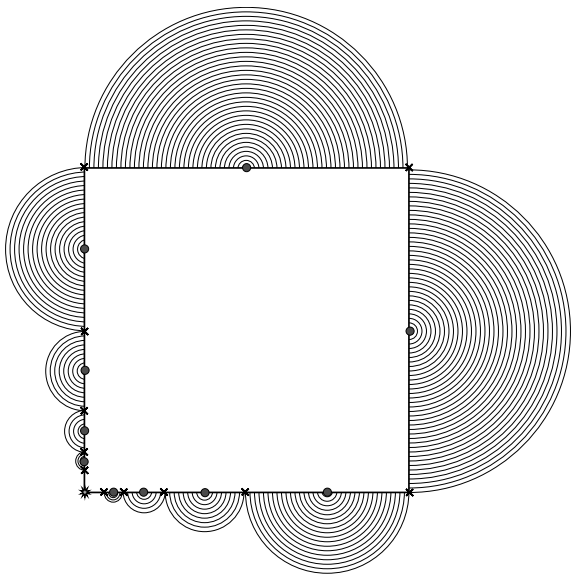


FIGURE 1. The side identifications that define the surface X.

Now we introduce identifications along the sides of $\tilde{X}$ in such a way that $\tilde{X}$ factors to a topological space X and $\tilde{f}$ factors to a self-homeomorphism of X. Except for points along the horizontal segment $0 < x < 1, y = \frac{1}{2}$, $\tilde{f}$ defines a self-mapping of $\tilde{X}$, and $\tilde{f}$ is discontinuous along this segment. On the one hand, if we regard this segment as lying on the boundary of X_1, its image by $\tilde{f}$ is the line segment $x + i, \frac{1}{2} < x < 1$ along the top of $\tilde{X}$, and on the other hand, if we regard it as lying on the boundary of X_0, its image by $\tilde{f}$ is the line segment $x + i, 0 < x < \frac{1}{2}$. Hence, in order to make $\tilde{f}$ continuous and well defined along this segment, in the construction of X we identify the points $\frac{1}{2} \pm t + i$ for $0 < t < \frac{1}{2}$ along the top of $\tilde{X}$.

Similarly, since $\tilde{f}$ maps the two points $1 + i(\frac{1}{2} \pm t), 0 < t < \frac{1}{2}$ along the right-hand edge of $\tilde{X}$ to the same point in the interior of $\tilde{X}$, in order to make $\tilde{f}$ one-to-one we identify these two points.

Now the top edge of $\tilde{X}$ is mapped by $\tilde{f}$ to the interval $\frac{1}{2} < x < 1, y = 0$. This means that for f to be well defined we must identify the points $x = \frac{3}{4} \pm t, y = 0$ for $0 < t < \frac{1}{4}$. Similarly, the vertical interval $\frac{1}{2} < y < 1, x = 0$ is mapped to $0 < y < 1, x = 1$, so for f to be one-to-one we must identify the points $y = \frac{3}{4} \pm t, x = 0$ for $0 < t < \frac{1}{4}$. By considering higher and higher compositions of $\tilde{f}$ with itself, we are led to the subdivision of the sides of the unit square shown in Figure 1. The points marked with $\times$'s indicate the boundaries of the intervals, and the totality of these points comprise the set $\mathcal{S}$ that is taken out of the closed unit square to form $\tilde{X}$. The dots indicate the midpoints of these intervals. We call these dots *hinge* points because for such points p on horizontal intervals the identification identifies $p+t$ with $p-t$ and for such points on vertical intervals it identifies $p + it$ with $p - it$. The steps defining $\tilde{f}$ are illustrated in Figures 1 and 2 and the hinge points appear as bold dots along the boundary of the square $\tilde{X}$.

https://doi.org/10.1017/S0143385706000484 Published online by Cambridge University Press

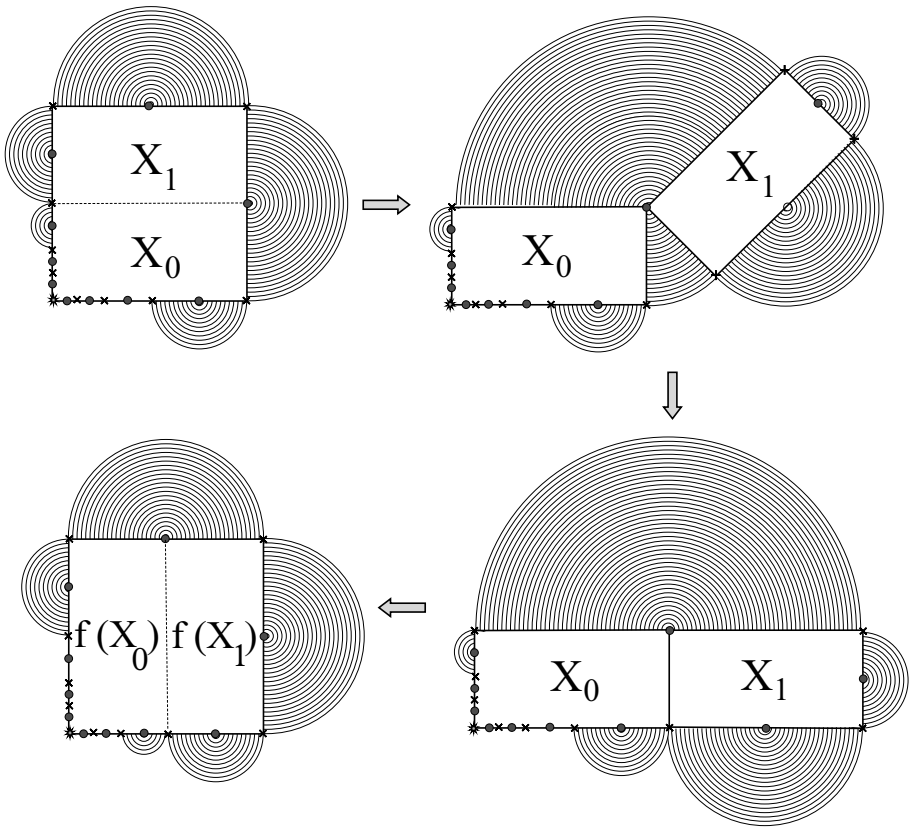


FIGURE 2. The horseshoe self-map $\tilde{f}$ of $\tilde{X}$.

The following theorem is a consequence of Theorem 20 of de Carvalho and Hall in [**4**]. We also refer to [**3**].

THEOREM 1. *X is a Riemann surface of genus zero and, as such, by Koebe's uniformization theorem, is conformally embeddable in the complex plane. Up to post-composition by an affine transformation, the embedding is unique. In particular, the embedding maps X onto $\mathbb{C}$.*

Proof. From the picture in Figure 1 with the semicircular regions added to the boundary intervals on $\tilde{X}$ to indicate the identifications by which X is formed from $\tilde{X}$, it is clear that X is of planar type in the sense that any simple closed curve in X separates X into two components. Therefore X is a non-compact, genus zero Riemann surface and so can be holomorphically embedded into $\mathbb{C}$.

Let ζ be the complex parameter in X and let z be the image of ζ under such an embedding. If p is a hinge point on the boundary of $\tilde{X}$, clearly the family Γ_p of semicircles in $\tilde{X}$ with central point at a hinge point p and radius less than half the length of the interval I_p of which p is the midpoint forms a curve family with zero extremal length in X. Therefore, $z(\Gamma_p)$ must also have zero extremal length in $\mathbb{C}$ and z extends to a holomorphic local homeomorphism at p.

https://doi.org/10.1017/S0143385706000484 Published online by Cambridge University Press

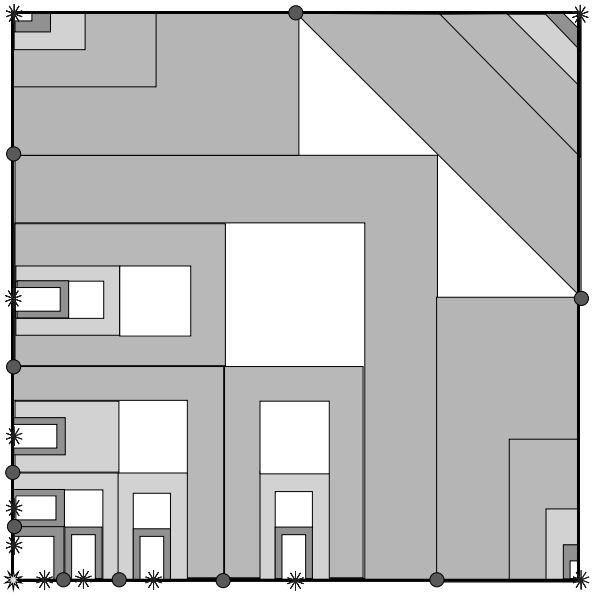


FIGURE 3. The sequence of nested annuli A_p surrounding the points $x_p, x_{p+1}, \ldots$.

The next step is to find a sequence of nested annuli A_p that surround the points x_p which are the endpoints of the intervals I_p with the property that the sum of the moduli of A_p diverges. It is enough to show that if we view the entire set of such endpoints as a single point q, then $z(q)$ is an isolated point in the Riemann sphere, which we may normalize to be ∞. Moreover, with this normalization the map $\zeta \mapsto z$ is unique up to post-composition with an affine map. The proof that the sum of these moduli diverges is postponed to §4, where it is shown that the extremal length across each annulus A_n is greater than a constant times $1/n$. Figure 3 shows A_1, A_2, A_3 and A_4. □

1.2. *The baker example.* The baker example is created by following a procedure similar to that followed in the horseshoe example. We start with the rectangle $\tilde{Y} = \{(x, y) : 0 \leq x \leq 1, 0 \leq y \leq 2\}$ minus a set $\mathcal{S}$, where once again $\mathcal{S}$ is a countable set on the boundary of $\tilde{Y}$, but now with two accumulation points. The exact locations of the points of $\mathcal{S}$ are dictated by the action of a new homeomorphism F of Y, which is defined by first defining a discontinuous map $\tilde{F}$ on $\tilde{Y}$. The baker example differs from the horseshoe example in that we work with a rectangle instead of a square and when we shift the top half Y_1 to the right and downwards, and place it next to Y_0; we do not turn it over.

More precisely, let $Y_0 = \{(x, y) : 0 \leq x \leq 1, 0 \leq y \leq 1\}$ and $Y_1 = \{(x, y) : 0 \leq x \leq 1, 1 \leq y \leq 2\}$. $\tilde{F}$ is defined in two steps as follows. First cut off the top half Y_1 and shift it to the right and down by the transformation $L(z) = z + 1 - i$. Then glue these two rectangular pieces together along the vertical line segment $x = 1, 0 < y < 1$, and apply the map $x + iy \mapsto (\frac{1}{2})x + 2iy$. This yields a self-mapping $\tilde{F}$ of $\tilde{Y} = Y_0 \cup Y_1$. Once again, we impose identifications along the sides of $\tilde{Y}$ to create Y which make $\tilde{F}$

https://doi.org/10.1017/S0143385706000484 Published online by Cambridge University Press

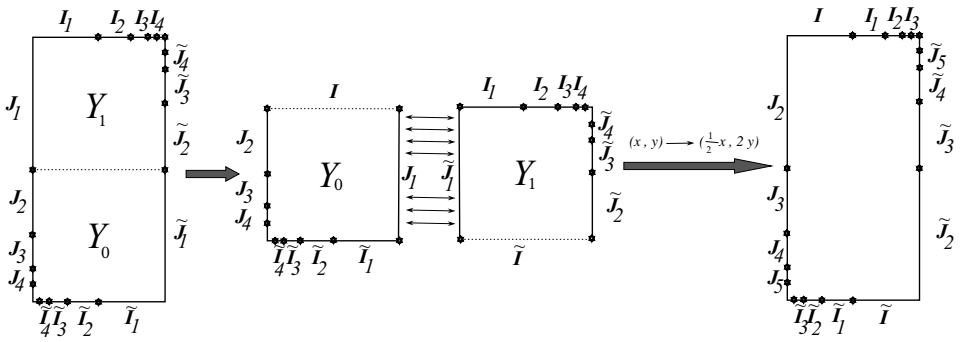


FIGURE 4. The baker self-map F of Y.

factor to a homeomorphism F of Y. Figure 4 illustrates $\tilde{F}$ in two steps. In the first step the top half Y_1 is translated by $z \mapsto z + 1 - i$. In the second step the resulting rectangle is compressed by a factor of $1/2$ in the horizontal direction and expanded by a factor of 2 in the vertical direction. The intervals I_k and J_k are identified with the intervals $\tilde{I}_k$ and $\tilde{J}_k$ by pure translations.

THEOREM 2. *Let c be the conformal self map of Y defined by rotation by* 180° *around the point $\frac{1}{2} + i$. Then the factor space Y/c is naturally isomorphic to X and the self-homeomorphism f of X lifts to the self-homeomorphism F of Y. Y is an infinite genus degree two cover of X ramified of order two over each of the hinge points of X.*

Proof. $c(\zeta) = -\zeta + 1 + 2i$ is the conformal self-map of $\tilde{Y}$ that represents the 180° rotation around the point $\frac{1}{2} + i$. Clearly, the boundary identifications of $\tilde{Y}$ are preserved by c and so c factors to a conformal self-map Y. We denote this factor map by the same letter, c (see Figure 5). Since $c(\frac{1}{2} \pm t + i) = \frac{1}{2} \mp t + i$, the points $\frac{1}{2} \pm t + i$, for $0 < t < \frac{1}{2}$, are identified. Y_0 forms a fundamental domain for the action of c on Y. Moreover, the translation identifications on the sides of $\tilde{Y}$ combined with c induce all of the hinge point identifications on the sides of X. For example, consider the map $L(\tilde{\zeta}) = \zeta - \frac{1}{2} + 2i$ which identifies the interval $\frac{1}{2} < x < 1, y = 0$ on the bottom of $\tilde{Y}$ with the interval $0 < x < \frac{1}{2}, y = 2$ on the top of $\tilde{Y}$. Then $c \circ L(\zeta) = -\zeta + \frac{3}{2}$, which is rotation by 180° around the point $\frac{3}{4}$, and if $L(\zeta) = \zeta - 1 + i$, and $c \circ L(\zeta) = -\zeta + 2 + i$, which is rotation by 180° around the point $1 + i/2$. The upshot is that the transformations $c \circ L$ where L varies through the side identifications on $\tilde{Y}$ generate all of the order-two side identifications on $\tilde{X}$, which can be identified with Y_0. In particular, this shows that the cover of Y is ramified of order two over the hinge points of X.

To see that Y has infinite genus, we leave it to the reader to construct an infinite family of pairs of closed curves $\{\alpha_j, \beta_j\}_{j=1}^{\infty}$ with the following properties:

(1) all of the curves α_j and β_j are simple;
(2) α_j does not intersect any other α_k or β_k except for β_j;
(3) β_j does not intersect any other α_k or β_k except for α_j;
(4) for every j, α_j intersects β_j at exactly one point;
(5) no two of the curves in the family $\{\alpha_j, \beta_j\}$ are homotopic. □

https://doi.org/10.1017/S0143385706000484 Published online by Cambridge University Press

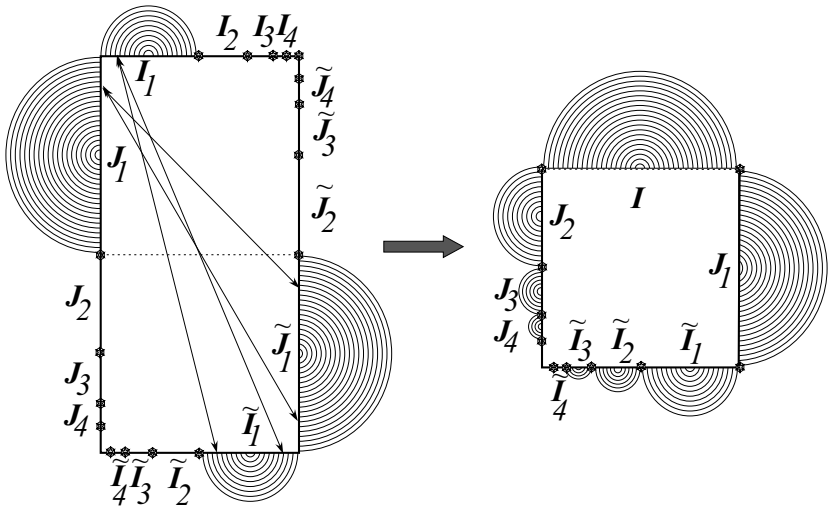


FIGURE 5. Y is a degree two cover of X ramified of order two over each of the hinge points of X.

2. *Surfaces generated by affine side pairings*

In this section we make only a finite number of side identifications along the sides of a closed rectangle $\tilde{Y}$ with horizontal and vertical sides in the complex ζ-plane $\mathbb{C}$. Each of the horizontal sides of $\tilde{Y}$ is subdivided into n subintervals and the vertical sides into m subintervals. The subintervals along the bottom of $\tilde{Y}$ are labeled from left to right by $\{I_k\}_{k=1}^n$ and the intervals along the top of $\tilde{Y}$ are labeled *in reverse order* from right to left by $\{\tilde{I}_k\}_{k=1}^n$. Similarly, the intervals along the left-hand vertical side of $\tilde{Y}$ are labeled from bottom to top by $\{J_k\}_{k=1}^m$ and along the right-hand vertical side of $\tilde{Y}$ by $\{\tilde{J}_k\}_{k=1}^m$ *in reverse order* from top to bottom. Moreover, we assume that the lengths of I_k and $\tilde{I}_k$ are equal, and similarly the lengths of J_k and $\tilde{J}_k$ are equal.

Consider the topological space Y_{nm} obtained from $\tilde{Y}$ by identifying I_k with $\tilde{I}_k$ and J_k with $\tilde{J}_k$ by translations. At points in the interior of $\tilde{Y}$ it is obvious that the complex parameter ζ of $\tilde{Y} \subset \mathbb{C}$ induces a conformal structure on Y_{nm}. At points on the boundary of $\tilde{Y}$ but in the interior of one of the boundary intervals, the translations identifying I_k with $\tilde{I}_k$ or J_k with $\tilde{J}_k$ give transition functions that determine the conformal structure at these points as well. One can also introduce a local parameter at the point or points determined by the endpoints of these intervals, as is explained in the following theorem.

THEOREM 3. *With the identifications described above, Y_{nm} inherits from $\tilde{Y}$ the structure of a compact Riemann surface of genus $(n+m)/2$ if $n+m$ is even and $(n+m-1)/2$ if $n+m$ is odd. The differential $d\zeta$ is an abelian differential on Y_{nm} which is non-vanishing except at one or two points. If $n+m$ is even, $d\zeta$ has a single zero of order $n+m-2$, and if $n+m$ is odd, $d\zeta$ has two zeros each of order $(n+m-3)/2$.*

Proof. The side-pairings of the specified intervals along the sides of $\tilde{Y}$ induce an identification of the endpoints of these intervals. We leave it to the reader to check that in the case that $n+m$ is even, all of these endpoints are identified to a single point, and in the case that $n+m$ is odd, the endpoints of these intervals divide into two cycles.

https://doi.org/10.1017/S0143385706000484 Published online by Cambridge University Press

First, assume $n + m$ is even. For each of these endpoints p, choose a semi-disk or quarter disk formed by taking the intersection of a small circle centered at p with the rectangle $\tilde{Y}$. By translating and rotating, move these regions so that their centers are moved to zero in the $\zeta-$plane and so that successively identified sides are adjacent. There are $2m+2n-4$ of these regions subtend π radians and four of them come from the four vertices of the rectangle $\tilde{Y}$ subtend $\pi/2$ radians. Therefore, the total angle in the ζ-parameter is $(n + m - 1) \times 2\pi$ radians, and a local parameter t may be introduced by the formula

$$t^{n+m-1} = \zeta. \tag{5}$$

Therefore, $d\zeta = (n+m-1)t^{n+m-2}dt$ and $d\zeta$ has a single zero of order $n+m-2$. Since, in general, an abelian differential on a compact Riemann surface has order equal to twice the genus minus two, this shows that Y_{nm} has genus $(n + m)/2$.

Second, assume $n+m$ is odd. Then the side-pairing identifications yield two equivalence classes of their $2m + 2n$ endpoints. Each of these equivalence classes contains $m + n$ points, and in each equivalence class there are two points that subtend $\pi/2$ radians and $m + n - 2$ points that subtend π radians. The two equivalence classes yield two points on the surface Y at which we introduce local parameters s and t. After appropriate rotations and translations in ζ, we have

$$\zeta = s^{(m+n-1)/2} \quad \text{and} \quad \zeta = t^{(m+n-1)/2}.$$

Thus

$$d\zeta = \frac{(m+n-1)}{2}s^{(m+n-3)/2} \quad \text{and} \quad d\zeta = \frac{(m+n-1)}{2}t^{(m+n-3)/2}.$$

So $d\zeta$ has two zeros on Y each of order $(m + n - 3)/2$, and the net number of zeros of $d\zeta$ is $m + n - 3$. By solving $2g - 2 = m + n - 3$ we find that the genus of Y is equal to $(m + n - 1)/2$. □

3. *The hyperelliptic cover*

Let p_0 be the center point of the rectangle $\tilde{Y}$, that is, p_0 is the intersection of the diagonals of $\tilde{Y}$. Let $C(\zeta) = -(\zeta - p_0) + p_0 = -\zeta + 2p_0$: that is, C is the conformal rotation of order two around the point p_0. Note that if two points p in I_k and q in $\tilde{I}_k$ are identified by the translation taking I_k to $\tilde{I}_k$, then $C(p)$ and $C(q)$ are points in $\tilde{I}_k$ and I_k identified by the same translation. Of course a similar statement is true for points in J_k and $\tilde{J}_k$, and thus C induces a conformal involution c of Y_{nm}.

The quotient Riemann surface $Y_{nm}/c \cong X_{nm}$ can be viewed as obtained from side-identifications on a fundamental domain for c. As a fundamental domain we choose the right triangle T with the hypotenuse equal to the diagonal connecting the upper-left corner of $\tilde{Y}$ to its lower-right corner and its two legs equal to the left and bottom sides of $\tilde{Y}$. The translations that identify I_k with $\tilde{I}_k$ and J_k with $\tilde{J}_k$ together with C generate 180° rotations about the central points of each one of the intervals I_k,J_k, and the hypotenuse of T. Each of these intervals factored by a rotation about its midpoint yield side-pairing identifications on contiguous intervals that form the entire boundary of T, and T factored by these identifications forms a Riemann surface of genus zero isomorphic to X. One can easily see that T with these side identifications has genus zero by the same reason given

https://doi.org/10.1017/S0143385706000484 Published online by Cambridge University Press

in the first paragraph of the proof of Theorem 1. If we let ζ be the complex parameter in T, by Koebe's uniformization theorem, there is a conformal map $\zeta \mapsto z_{nm}$ mapping T to $\mathbb{C} \cup \{\infty\}$, and with the property that points identified on the boundary of T are mapped to the same point by $\zeta \mapsto z_{nm}$. Let p_j be the midpoint of I_j, q_k be the midpoint of J_k, and ζ_0 be the midpoint of the hypotenuse of T. Also put $z(p_j) = a_j$, $z(q_k) = a_{-k}$ and $z(p_0) = a_0$.

THEOREM 4. *The map $\zeta \mapsto z_{nm}$ from X_{nm} to $\mathbb{C} \cup \{\infty\}$ is unique up to post-composition by a Möbius transformation. Moreover, $(d\zeta)^2$ induces on $\mathbb{C} \cup \{\infty\}$ a meromorphic quadratic differential with simple poles at the points $p_j, 0 \le j \le n$, and $q_k, 1 \le k \le m$ and a zero of order $m+n-3$ at the point corresponding to the image of the endpoints of the intervals I_j and J_k.*

Proof. Note that for any hinge point p we identify $\zeta_1 = p + t$ with $\zeta_2 = p - t$ where $p \pm t$ are in the same horizontal side interval, and we identify $\zeta_1 = p + it$ with $\zeta_2 = p - it$ where $p \pm it$ are in the same vertical side interval. In either case $\zeta_1 = -\zeta_2 + 2p$ and so $(d\zeta)^2$ is a well-defined quadratic differential on X_{nm}. Also, for any hinge point p, $t = (\zeta - p)^2$ is a local parameter for X_{nm} that vanishes at $\zeta = p$. Thus, $dt = 2(\zeta - p)d\zeta$, $(dt)^2 = 4(\zeta - p)^2(d\zeta)^2 = 4t(d\zeta)^2$. Therefore,

$$(d\zeta)^2 = (4t)^{-1}(dt)^2,$$

and so $(d\zeta)^2$ has a simple pole at $t = 0$. Since there are n hinge points along the bottom of T, m hinge points on the left side of T and one hinge point on the hypotenuse, altogether $(d\zeta)^2$ has $m+n+1$ simple poles. The endpoints of the intervals I_j and J_k are identified to a single point on X_{nm} at which $(d\zeta)^2$ has a high order zero. For reasons which will become clear from the dynamical application we shall call this point the *umbilic point*. To calculate the order of this zero, at each one of these endpoints x we apply a coordinate chart of the form $t = e^{i\theta}(\zeta - x)^\alpha$ where $\theta = \theta(x)$ is chosen so that these charts paste together onto a neighborhood of zero in the t-plane. Observe that in the ζ-plane there is one endpoint where the angle is $\pi/2$, two endpoints where the angle is $\pi/4$ and $(m-1)+(n-1)$ endpoints where the angle is π. Therefore, the net angle is $(m+n-1) \times \pi$. Thus, in each sector

$$\zeta - x = (te^{-i\theta(x)})^{(m+n-1)/2} \quad \text{and} \quad (d\zeta)^2 = \lambda\left(\frac{m+n-1}{2}\right)^2 t^{m+n-3}(dt)^2, \qquad (6)$$

where λ is a complex number with absolute value 1. So the only zero of $(d\zeta)^2$ has order $m+n-3$.

Since by adding these local parameters at the hinge points and at the umbilic point we have provided a system of charts on X making it into a compact Riemann surface of genus zero, X is isomorphic to $\mathbb{C} \cup \{\infty\}$ and this isomorphism is unique up to postcomposition by a Möbius transformation. □

THEOREM 5. *Let $\zeta \mapsto z$ be normalized so that the image of the umbilic point is the point at infinity and the image of p_0 is 0. Furthermore, assume that in terms of the local parameter $t = (\zeta - p_0)^2$*

$$\left.\frac{dz}{dt}\right|_{t=0} = 1/4.$$

https://doi.org/10.1017/S0143385706000484 Published online by Cambridge University Press

Define w_{nm} by $w_{nm} = dz_{nm}/d\zeta$. Then w_{nm} is a meromorphic function on Y_{nm}, w_{nm}^2 is a well-defined function of z_{nm} on X_{nm} and

$$w_{nm}^2(z_{nm}) = z_{nm}\left(\prod_{j=1}^{n}\left(1 - \frac{z_{nm}}{z_{nm}(p_j)}\right)\right)\left(\prod_{k=1}^{m}\left(1 - \frac{z_{nm}}{z_{nm}(q_k)}\right)\right). \tag{7}$$

Proof. We have seen that Y_{nm} is a surface of genus depending on m and n, and there is a conformal involution c of Y_{nm} with p_0 as fixed point with the property that $Y_{nm}/c \cong X_{nm}$. We think of Y_{nm} as obtained from a rectangle $\tilde{Y}$ in the first quadrant of the ζ-plane with its bottom side on the horizontal axis and its left side along the vertical axis. Identifications of intervals along the sides of $\tilde{Y}$ given by translations realize Y_{nm} as a factor space. The lower left triangle T is obtained from $\tilde{Y}$ by cutting along the diagonal of $\tilde{Y}$ which goes from its upper left vertex to the lower right vertex. Then X is obtained from T by making certain identifications along the sides of T realized by compositions of translations and 180° rotations. Since the identifications of the sides of $\tilde{Y}$ involve only translations, $d\zeta$ is a well-defined abelian differential on Y_{nm}, and since the identifications for T involve only translations and 180° rotations $(d\zeta)^2$ is a well-defined meromorphic quadratic differential on X.

Since $w_{nm} = dz_{nm}/d\zeta$ is a meromorphic function on Y_{nm} and w_{nm}^2 is well-defined on X_{nm}, under the isomorphism of X_{nm} with $\mathbb{C} \cup \{\infty\}$, w_{nm}^2 is a function of $z_{nm} \in \mathbb{C}$. Although w_{nm} and z_{nm} depend on the n and m side identifications, for simplicity of notation in the following calculations we drop the subscripts n and m.

First we calculate the orders of the zeros and poles of $w^2(z)$. A local parameter t vanishing at a hinge point p, where $p = p_j$ or q_k, is given by

$$t = (\zeta - p)^2,$$

so $dt = 2(\zeta - p)d\zeta$ and

$$w = \frac{dz}{d\zeta} = \frac{dz}{dt}\frac{dt}{d\zeta} = 2(\zeta - p)\frac{dz}{dt} \quad \text{and} \quad w^2 = 4t\left(\frac{dz}{dt}\right)^2.$$

Since dz/dt does not vanish at $t = 0$, the last equation shows that $w^2(z)$ has a simple zero at the value of z corresponding to $t = 0$, which is $z(p)$, and explains all of the factors appearing in equation (7). It remains to show that the product in equation (7) has the correct order at ∞ and the correct normalization. Let $\tilde{z} = 1/z$ be a local parameter on the sphere vanishing at $z = \infty$. Then

$$\left(\frac{dz}{d\zeta}\right)^2 = \left(\frac{dz}{d\tilde{z}}\frac{d\tilde{z}}{dt}\frac{dt}{d\zeta}\right)^2.$$

Now $(dz/d\tilde{z})^2$ has a pole of order four at $z = \infty$, from equation (6) $(dt/d\zeta)^2$ has a pole of order $n + m - 3$ at $z = \infty$, and by definition $d\tilde{z}/dt$ is holomorphic and non-vanishing at $z = \infty$. Therefore, the order of the pole of w^2 at $z = \infty$ is $n + m + 1$, which is equal to the number of factors on the right-hand side of equation (7). Thus $w^2(z)$ vanishes at $z = 0$ and maps ∞ to ∞.

To check the normalization we must calculate the first derivative of w^2 with respect to z at $z = 0$. Note that $dz/d\zeta$ is defined only up to a plus or minus sign at p_0 but that its

https://doi.org/10.1017/S0143385706000484 Published online by Cambridge University Press

second derivative is invariantly defined. We find that

$$\frac{d(w^2)}{dz} = 2w\frac{dw}{dz} = 2w\frac{dw}{d\zeta}\frac{d\zeta}{dz} = 2\frac{dw}{d\zeta} = 2\frac{d^2z}{d\zeta^2} = 2\left(\frac{d}{d\zeta}\frac{dz}{dt}\right)\frac{dt}{d\zeta} + 2\frac{dz}{dt}\frac{d^2t}{d\zeta^2}. \quad (8)$$

Since $t = (\zeta - p_0)^2$, the first term $dt/d\zeta$ in this last line is equal to zero when evaluated at $\zeta = p_0$ and, by the normalization $dz/dt|_{t=0} = \frac{1}{4}$, the second term is equal to 1.

Since they have the same normalization and zeros and poles of the same order at the same positions, this proves the left- and right-hand sides of equation (7) are equal. □

COROLLARY 1. $(d\zeta)^2$ *determines a meromorphic quadratic differential on* $\mathbb{C} \cup \{\infty\}$ *of finite norm and*

$$(d\zeta)^2 = \frac{(dz_{nm})^2}{z_{nm}\left(\prod_{j=1}^{n}(1 - z_{nm}/z_{nm}(p_j))\right)\left(\prod_{k=1}^{m}(1 - z_{nm}/z_{nm}(q_k))\right)}. \quad (9)$$

4. *The estimate*

Now assume the number m of intervals J_k is equal to the number n of intervals I_j. By Theorem 3 this means that $d\zeta$ determines an abelian differential on Y_{nn} with a single zero of order $2n - 2$ and that Y_{nn} has genus n. Also choose the intervals I_j and J_k to be of the special form similar to the intervals generated by the horseshoe example. Specifically, let J_1 be the line segment $[i/2, i]$, $J_2 = [i/4, i/2], \ldots, J_n = [0, i/2^{n-1}]$. For J_k with negative subscripts, let $J_{-1} = I_1 = [\frac{1}{2}, 1]$, $J_{-2} = I_2 = [\frac{1}{4}, \frac{1}{2}], \ldots, J_{-n} = [0, 1/2^{n-1}]$. Finally, let J_0 be the diagonal line segment joining 1 to i. Since we have chosen m equal to n, to simplify notation we denote X_{nn}, Y_{nn}, z_{nn} and w_{nn} by X_n, Y_n, z_n and w_n, respectively. Note that for each n, $\tilde{X}$ factored by the equivalence relation identifying points on its sides is isomorphic to the complex sphere. The isomorphism $\zeta \mapsto z_n$ is uniquely determined by the normalization specified in Theorem 5.

If we let a_{kn} be the image of the midpoint of J_k under the map $\zeta \mapsto z_n$ and $w_n = dz_n/d\zeta$, then formulas (7) and (9) take the form

$$w_n^2(z) = z_n \prod_{|k|=1}^{n}\left(1 - \frac{z_n}{a_{kn}}\right) \quad (10)$$

and

$$(d\zeta)^2 = \frac{(dz_n)^2}{w_n^2} = \frac{(dz_n)^2}{z_n\left(\prod_{|k|=1}^{n}(1 - z_n/a_{kn})\right)}. \quad (11)$$

We have chosen the labelling so that as k increases from $-n$ to n, the intervals J_k surround the triangle T starting at the lower left vertex and moving around T in the counterclockwise direction. By using Figure 4, we will construct a family of nested topological annuli $A_1, \ldots, A_n$ on X with the following properties:

- the complement of every annulus A_k, $1 \le k \le n$, contains in one component the umbilic point and in the other component $\{p_{-2}, p_{-1}, p_0, p_1\}$;
- for each k, the component of the complement which contains p_0 also contains $\{p_{-k-1}, \ldots, p_k\}$;

https://doi.org/10.1017/S0143385706000484 Published online by Cambridge University Press

- the annuli are nested in the sense that A_{k+1} is contained in the component of the complement of A_k which contains the umbilic point.

To obtain these annuli, first change the triangle T to a rectangle $\tilde{X}$ by cutting off the subtriangle to the right of the vertical line $\xi = \frac{1}{2}$ and rotating it 180° around the hinge point $p_0 = (1 + i)/2$. Then apply the map $\zeta = \xi + i\eta \mapsto 2\xi + i\eta$ to convert this rectangle to a square S, which coincides with the square shown in Figure 3. Note that the side identifications on T induce side identifications on $\tilde{X}$ that yield the same Riemann surface X. Moreover, going around the square in the counterclockwise direction, the hinge points along the bottom are $p_{-n}, \ldots, p_{-2}$, p_0 is the midpoint of the right-hand side, p_{-1} is the midpoint of the top and $p_1, \ldots, p_n$ move from top down along the left hand side of S. We leave it to the reader to verify that the annuli $A_1, \ldots, A_{n-1}$ shown in Figure 3 have the required properties. Furthermore, by using $\rho(z) = 1$ as test metric for extremal length in the same manner as in [**5**, pp. 180–182], it follows that there are positive constants c_1 and c_2 such that the extremal length across the annulus A_n is greater than or equal to $1/(c_1 + c_2 n)$.

THEOREM 6. *Let $a_k = z(p_k)$. Then there are positive constants C and β such that for every positive integer n and every j with $|j| \geq n + 1$,*

$$n \leq C(|a_j| + 1)^{\beta}. \tag{12}$$

Proof. We shall use the following lemma from Ahlfors [**1**, p. 76, inequality (4-21)]. Suppose $\hat{A}$ is a topological annulus in $\mathbb{C}$ such that the bounded component of the complement of $\hat{A}$ contains 0 and 1 and the unbounded component contains z_0. Then

$$e^{2\pi\Lambda(\hat{A})} \leq 16(|z_0| + 1), \tag{13}$$

where $\Lambda(\hat{A})$ is the extremal length of the family of arcs in $\hat{A}$ that connect the inner component of its complement to the outer component.

Let $\hat{A}_n$ be the image of A_n under the conformal isomorphism $\zeta \mapsto z$, where $a_1 = z(p_1)$. Note that for all $n \geq 1$ the bounded component of $\hat{A}_n$ contains $\{a_{-n}, \ldots, a_n\}$, and all of the other points a_k are in the unbounded component of $\hat{A}_n$. Moreover, the annuli $\hat{A}_n$ are nested in the sense that each $\hat{A}_n$ is contained in the bounded component of the complement of $\hat{A}_{n+1}$. Let B_n be the annular domain whose complement has bounded component equal to the bounded component of the complement of $\hat{A}_1$ and unbounded component equal to the unbounded component of the complement of $\hat{A}_n$. Then the bounded component of B_n contains $\{a_{-1}, a_0, a_1\}$ and

$$\Lambda(B_n) \geq \sum_{k=1}^{n} \Lambda(\hat{A}_k) \geq \sum_{k=1}^{n} \frac{1}{cn} \geq (1/c)\log(n - 1),$$

where $c = c_1 + c_2$. It follows that for $|j| \geq n + 1$,

$$n \leq 16^{(c/2\pi)}(|a_j| + 1)^{(c/2\pi)},$$

so we may take $C = 16^{(c/2\pi)}$ and $\beta = (c/2\pi)$. □

COROLLARY 2. *In the case of the horseshoe example the points a_n converge to ∞ as n approaches $\pm\infty$.*

https://doi.org/10.1017/S0143385706000484 Published online by Cambridge University Press

Proof. In this case there are infinitely many intervals J_k running along the bottom of the triangle T for negative integers k and running along the left side of T for positive k. Since the estimate implies that $\Lambda(B_n) \to \infty$ as $n \to \infty$, the embedding $\zeta \mapsto z$ from T to $\mathbb{C}$ is surjective. It is therefore unique up to postcomposition by an affine transformation and

$$|a_k| \geq \frac{|k|^{2\pi/c}}{16} - 1$$

for positive and negative values of k. □

5. *The limiting product formula*

THEOREM 7. *The partial products*

$$w_n^2 = z_n \prod_{|k|=1}^{n} (1 - z_n/a_{kn}) \tag{14}$$

converge uniformly on compact sets of $\mathbb{C}$ *to* w^2.

Proof. Let $z_n(p_j) = a_{n,j}$, where z_n is the normalized uniformizing map from T with identifications on its sides up to level n onto $\mathbb{C}$, and let $w_n^2 = (dz_n/d\zeta)^2$. We consider the function $f_n(z) = z_n \circ z^{-1}(z)$. It is defined on that part of the z-plane which corresponds to points ζ in the interior of T and to points ζ on the boundary of T for which the equivalence relations determining X and X_n coincide. Moreover, it is a holomorphic function normalized with derivative equal to 1 at the origin and univalent on a disk of radius R_n, where from Theorem 6, $R_n \to \infty$ as $n \to \infty$. By Koebe's distortion theorem (see [**1**, p. 84]), for $|z| < R_n$,

$$\frac{|z|}{(1 + |z/R_n|)^2} \leq |f_n(z)| \leq \frac{|z|}{(1 - |z/R_n|)^2}, \tag{15}$$

and so $f_n(z)$ converges uniformly on all compact subsets of the plane to the identity. For use in the sequel we also note that Koebe's distortion theorem implies that

$$\frac{1}{(1 + |z/R_n|)^3} \leq |f_n'(z)| \leq \frac{1}{(1 - |z/R_n|)^3}. \tag{16}$$

It follows that $dz_n/d\zeta$ converges locally uniformly to $dz/d\zeta$ and therefore

$$w_n(z_n)^2 = z_n \prod_{|j|=1}^{n} (1 - z_n/a_{j,n}) \tag{17}$$

converges to w^2. □

By using the Lebesgue dominated convergence theorem, and Koebe's distortion theorem (15) and (16), we can improve Theorem 7 to a statement about L_1-convergence.

THEOREM 8. *The reciprocals of the partial products in formula (17) converge in the* L_1*-norm to* $1/w^2$*, where the* L_1*-norm is taken over any disk of the form* $\{z : |z| < R_0\}$ *in* $\mathbb{C}$.

https://doi.org/10.1017/S0143385706000484 Published online by Cambridge University Press

Proof. Let $G_n(z_n) = 1/w_n^2(z_n)$ and $G(z) = 1/w^2(z)$, and let $G_n^*(z) = G_n(f_n(z))f_n'(z)^2$. From the Jacobian change of variable formula, we know that

$$\iint_{\mathbb{C}} |G_n|\,dx_n\,dy_n = \iint_{\mathbb{C}} |G_n^*|\,dx\,dy = \iint_T d\xi\,d\eta = area(T), \tag{18}$$

where $area(T)$ is the Euclidean area of T. Similarly,

$$\iint_{\mathbb{C}} |G|\,dx\,dy = area(T). \tag{19}$$

Since G_n^* converges pointwise to G and since

$$\||G_n^* - G| - |G_n^*|\| \le |G|,$$

by the dominated convergence theorem we obtain

$$\iint_{\mathbb{C}} |G_n^* - G|\,dx\,dy - \iint_{\mathbb{C}} |G_n^*|\,dx\,dy \to -\iint_{\mathbb{C}} |G|\,dx\,dy.$$

Hence, from equations (18) and (19), we find that

$$\iint_{\mathbb{C}} |G_n^* - G|\,dx\,dy \to 0.$$

Consider the inequalities

$$\begin{aligned}
&\iint_{|z|<R_0} \left| \frac{1}{w^2(z)} - \frac{1}{z_n \prod_{|k|=1}^n (1 - z_n/a_{kn})} \right| dx\,dy \\
&\quad = \iint_{|z|<R_0} |G(z) - G_n(f_n(z))|\,dx\,dy \\
&\quad \le \iint_{|z|<R_0} |G(z) - G_n^*(z)|\,dx\,dy + \iint_{|z|<R_0} |G_n^*(z) - G_n(f_n(z))|\,dx\,dy \\
&\quad \le \iint_{|z|<R_0} |G(z) - G_n^*(z)|\,dx\,dy + \sup_{|z|<R_0} \{|1 - 1/f_n'^2(z)|\} \iint_{|z|<R_0} |G_n^*(z)|\,dx\,dy.
\end{aligned} \tag{20}$$

Since G_n^* converges to G in the L_1-norm, for sufficiently large n the last integral on the right-hand side in (20) is bounded by $\|G\| + 1$. Also, for sufficiently large n, R_n is so much larger than R_0 that from equation (16) the supremum in expression (20) can be made arbitrarily small. We conclude that

$$\iint_{|z|<R_0} \left| \frac{1}{w^2(z)} - \frac{1}{z_n \prod_{|k|=1}^n (1 - z_n/a_{kn})} \right| dx\,dy$$

approaches zero as $n \to \infty$. □

6. *The angle at the umbilic point*

In this section we make an observation about the trajectories of the quadratic differential $(d\zeta)^2 = (dz)^2/w^2$. The intervals I_j and J_k determine horizontal and vertical trajectories, which lead from simple poles of $(d\zeta)^2$ to the umbilic point. We call these trajectories

https://doi.org/10.1017/S0143385706000484 Published online by Cambridge University Press

the special trajectories. There is an obvious symmetry $\zeta \mapsto i\bar{\zeta}$ of T, which is reflection about the diagonal line segment joining 0 to $(1+i)/2$, and which preserves the side identifications on T. By a Möbius change of coordinates in the z-plane, we may take $z(p_0) = -1$, z(the umbilic point) $= 0$ and $\zeta \mapsto z$ takes the diagonal line segment in T joining $\zeta = 0$ to $\zeta = (1+i)/2$ to the part of the real axis in the z-plane which is to the right of 0 and to the left of -1, and finally, the hypotenuse of T to the unit line segment in the z-plane joining -1 to 0. Then the pushforward of the symmetry $\zeta \mapsto i\bar{\zeta}$ is complex conjugation in the z-plane.

THEOREM 9. *In the z-plane the special trajectories of $(d\zeta)^2$ all lead from the points a_j to the origin at the same angle, for negative j along horizontal trajectories, for positive j along vertical trajectories and for $j = 0$ along the diagonal trajectory in T leading from $\zeta = 0$ to $\zeta = (1+i)/2$.*

Proof. For the proof we refer to Figure 6 which shows the following features.

(1) The line segment from $z = -1$ to $z = 0$ is the image in the z-plane of the hypotenuse of the triangle T.
(2) The image of the midpoint of the hypotenuse, $\zeta = (1+i)/2$, is the point $z = -1$, and the umbilic point corresponds to $z = 0$.
(3) The image of the dotted line segment in T joining 0 to $(1+i)/2$ is the complementary part of the real axis, that is, $(\mathbb{R} \cup \{\infty\}) \setminus [-1, 0]$.
(4) The median of T at $\zeta = (1+i)/4$ corresponds to $z = \infty$.
(5) Although their location is not known, the points a_{-j} are drawn in the lower half plane with a_{-1} at $-i$ and a_{-j} at $-i/2^{j-1}$. Similarly, for positive subscripts, a_j is placed at $i/2^{j-1}$. Note that $\overline{a_j} = a_{-j}$.
(6) Although we do not know their exact shape or location, the image of the horizontal trajectories J_k for k negative are drawn as semicircles in the third quadrant joining a_k to the origin, and the image of the vertical trajectories J_k for k positive are drawn as semicircles in the second quadrant. Note that $\overline{z(J_k)} = z(J_{-k})$ and $z(J_0)$ is the interval from -1 to 0.

The conformal map $c : \zeta \mapsto (\frac{1}{2})\zeta$ is well defined for the equivalence relation on the two sides of T and therefore induces a conformal map of $(\mathbb{C} \cup \{\infty\}) \setminus [-1, 0]$ into itself which maps the special trajectories corresponding to intervals J_k or J_{-k} onto neighboring special trajectories corresponding to J_{k+1} or J_{-k-1}. Obviously, c has no fixed points in the interior of T and so its conjugate $\tilde{c} = z \circ c \circ (z)^{-1}$ has no fixed points in the interior of $z(T)$. If we think of $(\mathbb{C} \cup \{\infty\}) \setminus [-1, 0]$ as a model for the hyperbolic plane, then by Schwarz's lemma $\tilde{c}$ must be a weak contraction. Moreover, for positive k, $z(c(J_k)) = z(J_{k+1})$ and $z(c(J_{-k})) = z(c(J_{-k-1}))$. Since $c(T)$ is a subtriangle of T with hypotenuse joining $\frac{1}{2}$ to $\frac{i}{2}$, the image of $\tilde{c}$ is a subdomain of $(\mathbb{C} \cup \{\infty\}) \setminus [-1, 0]$ contained inside a closed curve made up of $z(c(J_1))$, $z(c(J_{-1}))$ and a simple arc invariant under complex conjugation and joining $z(p_1)$ to $z(p_{-1})$. Therefore, if $z(c(J_1))$ or $z(c(J_{-1}))$ were to meet the interval $[-1, 0]$ at a positive angle, then the image $\tilde{c}((\mathbb{C} \cup \{\infty\}) \setminus [-1, 0])$ would be a Bloch domain (see [**2**]), which would imply that $\tilde{c}$ has a fixed point in $(\mathbb{C} \cup \{\infty\}) \setminus [-1, 0]$. By repeating the same type of argument for the special trajectories $z(c(J_k))$ and $z(c(J_{-k}))$, we conclude that none of these angles can be positive. □

https://doi.org/10.1017/S0143385706000484 Published online by Cambridge University Press

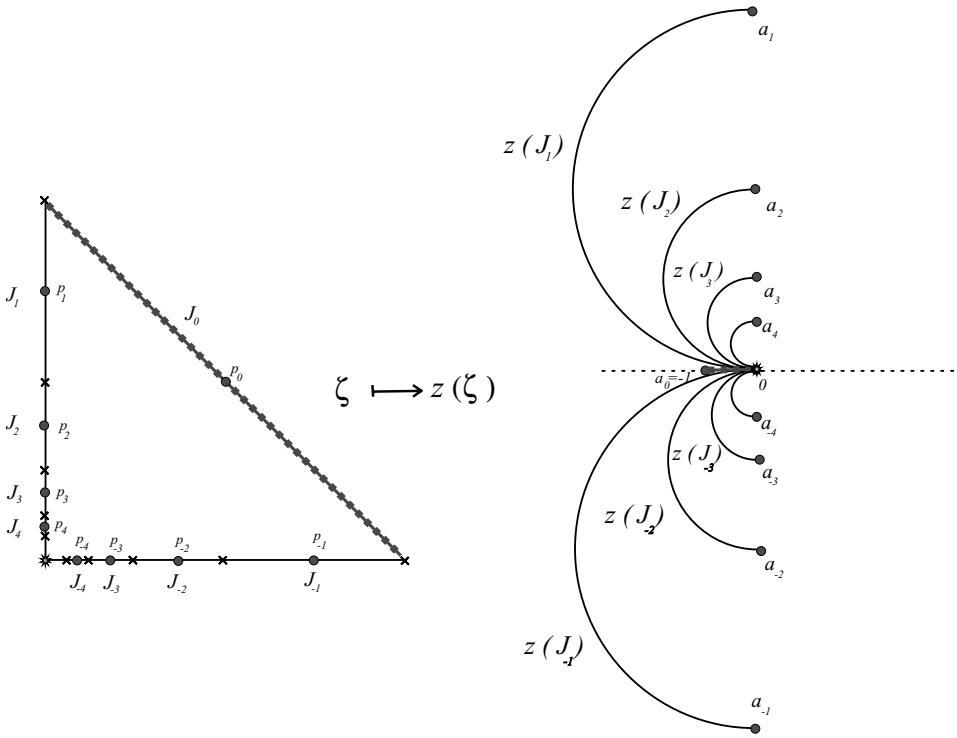


FIGURE 6. In the z-plane the special trajectories of the $(d\zeta)^2$ all lead from the points a_j to the origin at the same angle.

7. *A quasiconformal realization of X*

In this section we think of X as the triangle T with the appropriate side identifications. In the complex ζ-plane T has vertices at 0, 1 and i and hinge points at $3/2^n$, at $(3/2^n)i$ for any integer $n \geq 2$ and at $(1+i)/2$. We construct a piecewise quasiconformal map $\zeta \mapsto \tilde{z}$ from T into the complex $\tilde{z}$-plane such that the umbilic point corresponds to $\tilde{z} = \infty$ and such that the location of the hinge points and the images of the critical horizontal and vertical trajectories leading from the hinge points to the umbilic point are known. From this knowledge it is possible to make qualitative statements about their locations in the z-plane.

The strategy is to view $\zeta \mapsto \tilde{z}$ as a composition of three maps. The first is constructed from uniformly quasiconformal pieces and takes ζ to a domain in the w-plane that spirals around the origin infinitely many times. The second is given by $z_1 = \log w$, and the construction will show that z_1 is a one-to-one, well-defined function of ζ in T, except for values of ζ on the hypotenuse of T. The image $z_1(X)$ is the upper half-plane $\{z_1 = x_1 + iy_1 : y_1 \geq 0\}$. We will see that the conformal map $z_1 \mapsto \tilde{z} = z_1^2$ identifies all the points of the boundary of $z_1(T)$ which come from the same points of X.

To begin our construction we subdivide T in the ζ-plane into a disjoint union of two triangles and infinitely many trapezoids in the following way. First, we write T as the union of A and B where A is the triangle with vertices at 0, 1 and $(1+i)/2$ and B is the triangle

https://doi.org/10.1017/S0143385706000484 Published online by Cambridge University Press

with vertices at 0, i and $(1+i)/2$. Note that if j_ζ is reflection about the diagonal line passing through 0 and $1+i$, then $j_\zeta(A) = B$. Now we partition A into a union of sets A_N, where A_0 is the triangle with vertices at $1/2$, 1 and $(1+i)/2$, and for any integer $N \geq 1$, A_N is the trapezoid with vertices at $1/2^{N+1}$, $1/2^N$, $1/2^N + (1/2^N)i$, $1/2^{N+1} + (1/2^{N+1})i$. Similarly, B is the disjoint union of BN where $B_N = j_\zeta(A_N)$.

We define $\zeta \mapsto w$ piecewise on the regions A_N and B_N, $N \geq 0$. $N = 0$ is special case; A_0 maps onto the quarter disk $\tilde{A}_0$ lying in the first quadrant with its center at 0 and radius 1. The trapezoids A_N, for $N \geq 1$ map onto quarter disks $\tilde{A}_N$ with its center at 0 and radius 1 in other quadrants. In particular, A_1 maps into the second quadrant, A_2 to the third quadrant and in general A_N to the $(N+1)$th mod 4 quadrant. Consequently, A_N and A_{N+4} have the same image in the w-plane for $N \geq 1$.

To describe specifically the map, cut A_0 into four triangles by joining any pair of the points $\frac{3}{4}$, $\frac{1}{2} + (\frac{1}{4})i$, and $\frac{3}{4} + (\frac{1}{4})i$ with a straight line segment. (See the first drawing in Figure 7.) Going counterclockwise around the sides of A_0 we label the six points $c = \frac{1}{2}$, $j = \frac{3}{4}$, $k = 1$, $l = \frac{3}{4} + (\frac{1}{4})i$, $e = \frac{1}{2} + (\frac{1}{2})i$, and $d = \frac{1}{2} + (\frac{1}{4})i$. By definition, these six points in the ζ-plane are mapped to five points in the w-plane, $\tilde{c} = \tilde{k} = 0$, $\tilde{j} = \frac{1}{4} + (\frac{1}{4})i$, $\tilde{l} = 1$, $\tilde{e} = i$, $\tilde{d} = (\frac{1}{2})i$. In the triangles *cjd*, *jld* and *jkl* the map is real affine and in the triangle *led* the map is chosen so that it has the following features:

(1) it is quasiconformal;
(2) it maps the line segments *dl* and *de* linearly to the line segments $\tilde{d}\tilde{l}$ and $\tilde{d}\tilde{e}$;
(3) the line segment *le* is mapped onto the portion of the unit circle that is in the first quadrant.

To describe the map on the trapezoid A_1 label the midpoints of the sides of A_1 with the letters b, d, f and h, so that going counterclockwise around its boundary and starting at the lower left vertex the vertices and midpoints are labeled a through to h. Cut A_N into six triangles bounded by straight line segments *hb*, *hf*, *hd*, *bd* and *df*. The eight points a through to h are mapped to seven points in the portion of the unit disk that is in the second quadrant. We denote the images of these eight points by $\tilde{a}$ through to $\tilde{h}$ and we have $\tilde{a} = \tilde{c} = 0$, $\tilde{b} = -(\frac{1}{4}) + i(\frac{1}{4})$, $\tilde{d} = (\frac{1}{2})i$, $\tilde{e} = i$, $\tilde{f} = -(1/\sqrt{2}) + i(1/\sqrt{2})$, $\tilde{g} = -1$, $\tilde{h} = -(\frac{1}{2})$. Then we cut this quarter disk into six regions along the line segments $\tilde{h}\tilde{b}$, $\tilde{b}\tilde{d}$, $\tilde{b}\tilde{f}$, $\tilde{d}\tilde{f}$, $\tilde{f}\tilde{h}$ and the segment that joins $\tilde{b}$ to the origin. In general, the triangle in A_1 with vertices at xyz is mapped to the region with vertices at $\tilde{x}\tilde{y}\tilde{z}$. When the image region is also a triangle the mapping is assumed to be real affine and to map vertices to corresponding vertices. In the two cases when the image region has curvilinear boundary, that is, for the regions with vertices $\tilde{h}\tilde{g}\tilde{f}$ and $\tilde{f}\tilde{d}\tilde{e}$, we assume the map is quasiconformal, linear along the parts of the boundary which are straight line segments and maps x to $\tilde{x}$. We note that the points on the segments *ab* and *bc* on the boundary of A_1 that are identified are mapped to the same point along the segment joining $\tilde{b}$ to the origin in the quarter disk $\widetilde{A}_1$.

For $k \geq 1$ and $\zeta \in A_k$ we define the map by $w(\zeta) = i^{k-1} w(2^{k-1}\zeta)$. This puts the image $\widetilde{A}_2$ in the third quadrant, $\widetilde{A}_3$ in the fourth quadrant, $\widetilde{A}_4$ in the first quadrant, and so on. For $N \geq 1$, and $\zeta \in B_N$ we define $w(\zeta) = 1/\overline{w(j_\zeta(\zeta))}$. In this way w respects all the side identifications on T except for the one that identifies *le* with $j_\zeta(l)e$. In other words in the image of w, we must identify the segment $[0, 1]$ with $[1, \infty]$ by the map $w \mapsto (1/w)$.

https://doi.org/10.1017/S0143385706000484 Published online by Cambridge University Press

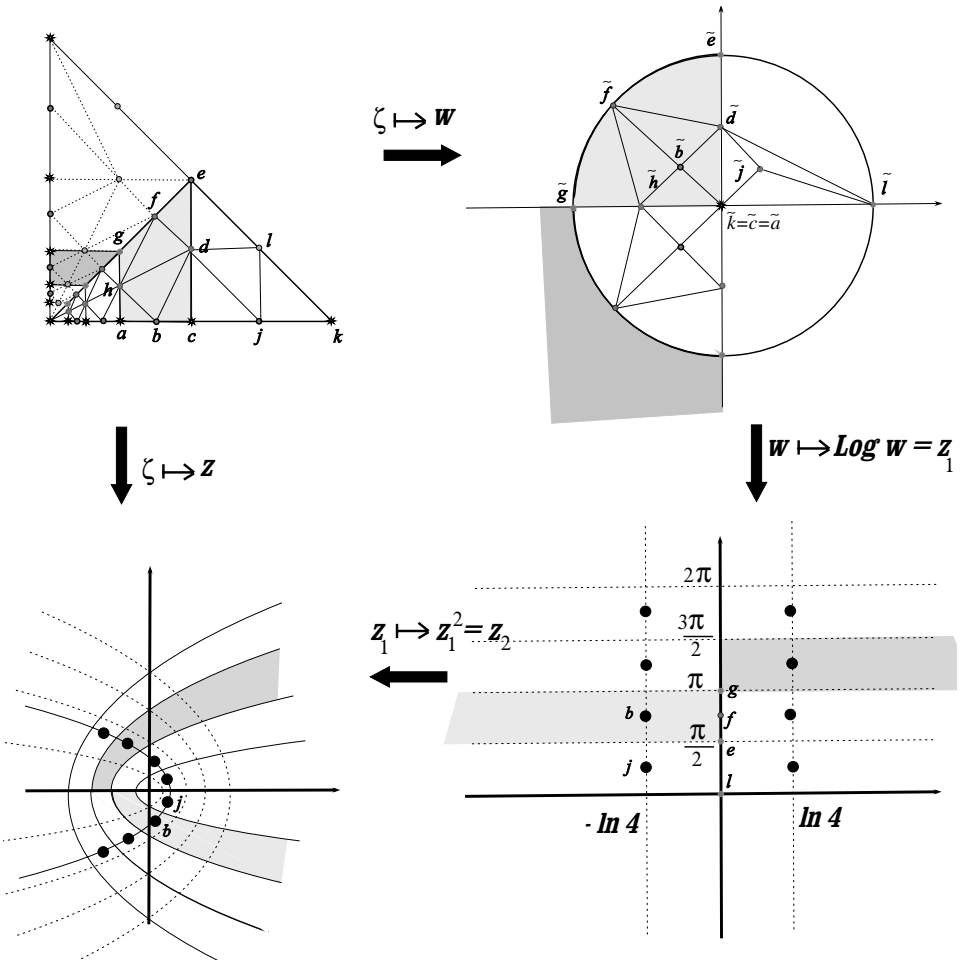


FIGURE 7. A quasiconformal realization of X.

Now we put $z_1 = \log w$. Then $z_1(\tilde{A})$ and $z_1(\tilde{B})$ lie in the first and second quadrants, and for $k \geq 0$, $z_1(\tilde{A}k)$ is the infinite half strip bounded by the vertical line segment from $k(\pi/2)i$ to $(k+1)(\pi/2)i$ and extending infinitely to the left. Similarly, for $k \geq 0$, $z_1(\tilde{B}k)$ is the infinite half strip bounded by the vertical line segment from $k(\pi/2)i$ to $(k+1)(\pi/2)i$ and extending infinitely to the right. The images of the hinge points P_{-k}, $k \geq 1$, are the points $\log(i^k \tilde{j}) = \log|\tilde{j}| + ((\pi/2) + k \arg \tilde{j})i = -\log 4 + ((2k+1)\pi/4)i$, and images of the hinge points P_k, $k \geq 1$, are the points $\log(i^k/(\bar{\tilde{j}})) = -\log|\tilde{j}| + ((\pi/2) + k \arg \tilde{j})i = \log 4 + ((2k+1)\pi/4)i$. Therefore, these images are periodic and located in each of the strips corresponding to A_N or B_N, $n \geq 0$. Notice that we still have to identify the positive real line with the negative real line by the map $z \mapsto -z$.

https://doi.org/10.1017/S0143385706000484 Published online by Cambridge University Press

Now form $\tilde{z} = z_1^2$, which collapses the boundary of $z_1(X)$ that maps points to be identified onto the same points of the positive real line. The images of the hinge points $p_k, k \in \mathbb{Z}, k \neq 0$, are the points

$$\tilde{a}_k = \log^2 4 - \frac{(2k+1)^2\pi^2}{16} + ((2k+1)(\log 2)\pi)i, \tag{21}$$

which all lie on the parabola $y^2 + 4(\log 4)^2 x - 4(\log 4)^4 = 0$.

In the next theorem we say that a sequence of points a_j converges to ∞ arithmetically if there exists positive constants α and C_1 and C_2 such that $C_1|j|^\alpha \geq |a_j| \geq C_2|j|^\alpha$.

THEOREM 10. *In the z-plane the sequence of hinge points converges to ∞ arithmetically.*

Proof. Let $a_j = z(\tilde{z}(z_1(w(p_k))))$ be the image of the hinge points in the z-plane. The result follows from formula (21) and from the facts that z is a quasiconformal function of ζ, $z(\infty) = \infty$, and z is a bi-Hölder continuous function of z_2 in the spherical metric. The positive constant α may be taken to be $1/K$ where K is the dilatation of the $\zeta \mapsto w$. □

Acknowledgements. The first author was partially supported by a grant from IPM (No. 83510120). The third author was partially supported by NSF grant 0200733.

REFERENCES

[1] L. V. Ahlfors. *Conformal Invariants: Topics in Geometric Function Theory*. McGraw-Hill, New York, 1973.

[2] A. Beardon, T. Carne, D. Minda, and P. Ng. Random iteration of analytic maps. *Ergod. Th. & Dynam. Sys.* **24**(3) (2004), 659–675.

[3] R. Chamanara. Affine automorphism groups of surfaces of infinite type. *In the Tradition of Ahlfors and Bers, III (AMS Contemp. Math. Ser., 355)*. American Mathematical Society, 2001, pp. 123–145.

[4] A. de Carvalho and T. Hall. Unimodal generalized pseudo-Anosov maps. *Geom. Topol.* **8** (2004), 1127–1188.

[5] C. J. Earle and F. P. Gardiner. Teichmüller disks and Veech's F-structures. *Contemp. Math.* **201** (1995), 165–189.

https://doi.org/10.1017/S0143385706000484 Published online by Cambridge University Press